

# SurveilEdge: Real-time Video Query based on Collaborative Cloud-Edge Deep Learning

1<sup>st</sup> Shibo Wang

School of Mathematics and Statistics  
Xi'an Jiaotong University  
wshb20081996@stu.xjtu.edu.cn

2<sup>nd</sup> Shusen Yang\*

School of Mathematics and Statistics  
Xi'an Jiaotong University  
shusenyang@mail.xjtu.edu.cn

3<sup>rd</sup> Cong Zhao

Department of Computing  
Imperial College London  
c.zhao@imperial.ac.uk

**Abstract**—The real-time query of massive surveillance video data plays a fundamental role in various smart urban applications such as public safety and intelligent transportation. Traditional cloud-based approaches are not applicable because of high transmission latency and prohibitive bandwidth cost, while edge devices are often incapable of executing complex vision algorithms with low latency and high accuracy due to restricted resources. Given the infeasibility of both cloud-only and edge-only solutions, we present SurveilEdge, a collaborative cloud-edge system for real-time queries of large-scale surveillance video streams. Specifically, we design a convolutional neural network (CNN) training scheme to reduce the training time with high accuracy, and an intelligent task allocator to balance the load among different computing nodes and to achieve the latency-accuracy tradeoff for real-time queries. We implement SurveilEdge on a prototype<sup>1</sup> with multiple edge devices and a public Cloud, and conduct extensive experiments using real-world surveillance video datasets. Evaluation results demonstrate that SurveilEdge manages to achieve up to  $7\times$  less bandwidth cost and  $5.4\times$  faster query response time than the cloud-only solution; and can improve query accuracy by up to 43.9% and achieve  $15.8\times$  speedup respectively, in comparison with edge-only approaches.

## I. INTRODUCTION

With the widespread deployment of surveillance cameras, the amount of surveillance video data has been increasing explosively. The IHS's 2019 report forecasts that over 180 million surveillance cameras will be shipped globally [1]. Since it is prohibitively costly and slow to extract information from consecutive surveillance videos with traditional manual manners, the automatic and intelligent video analytics has been attracting great attentions from both industry and academia [2] [3] [4].

An important application of video analytics is the real-time query of objects (e.g. car, people) within surveillance video streams, which are fundamental in various smart city applications such as event detection [5], target tracking [6], and intelligent traffic management [7] [8]. As illustrated in

This work was supported in part by the National Natural Science Foundation of China under Grant 61772410, Grant 61802298, and Grant U1811461, in part by National Key Research and Development Program of China under Grant 2017YFB1010004, in part by the China 1000 Young Talents Program, and in part by the Young Talent Support Plan of Xi'an Jiaotong University.

\* Corresponding author.

<sup>1</sup>The executable source code is available in the anonymous link <https://github.com/SurveilEdge/SurveilEdge>.

Fig. 1, a query task requires real-time responses of video frames containing the objects defined by the users (termed as query objects in the rest of the paper). This requires to process each video frame immediately when receiving it, which is different from offline video query applications (e.g., NoScope [2] and Focus [3]) that concentrate on queries of recorded video databases.

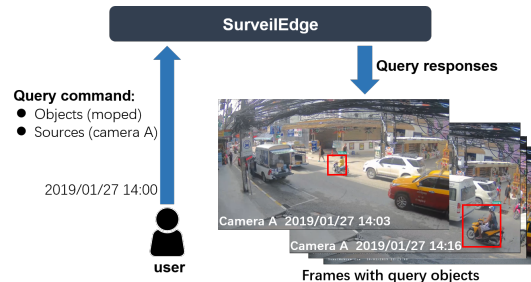


Fig. 1. An example of real-time surveillance video query. Users input the query command includes query objects (moped in this example), query locations (represented by camera IDs). The system response the output the video frames with query objects in real time.

The development of deep learning (especially CNNs [9]–[13]) has been promoting a breakthrough of video query applications [14]–[17], which are normally deployed on the Cloud to execute computation-intensive CNN algorithms (e.g. ResNet-152 [12] and Yolov3 [18]). Although Cloud-based solutions can guarantee high accuracy by using complex CNN models, they suffer from increasingly unaffordable bandwidth cost and large query latency due to the transmission of explosively growing surveillance video data.

Alternatively, the emerging edge computing paradigm [4] [19] enables to perform computation at edge devices, which can avoid raw video data transmission to the Cloud. However, most edge devices are resource-limited. As a result, they are only capable to deploy lightweight CNN models (e.g., MobileNet [20]), but are extremely inefficient (i.e., large computing latency) or even fail to perform complex CNN algorithms. Therefore, edge-based solutions cannot guarantee trustworthy query accuracy, especially considering that recalls are more crucial in practice.

By leveraging the advantages of Cloud computing and edge

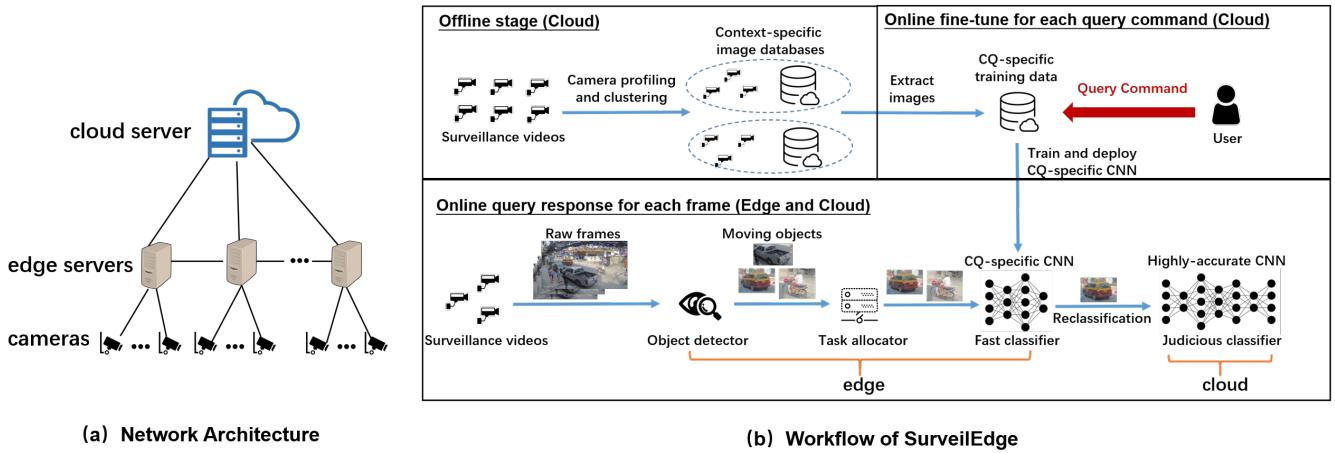


Fig. 2. The network architecture and workflow of SurveilEdge

computing in a collaborative way, we present SurveilEdge for real-time queries of large-scale surveillance video streams.

We build SurveilEdge and collect more than 170 hours of real-world surveillance videos from 14 cameras for performance evaluation. According to experimental results, SurveilEdge manages to achieve up to  $7\times$  fewer bandwidth cost and  $5.4\times$  faster query response time than the cloud-only solution; and can improve query accuracy by up to 43.9% and achieve  $15.8\times$  speedup respectively, in comparison with edge-only approaches.

- We combine the characteristics of surveillance videos we observed with the fine-tuning technique to train specific CNNs, which significantly reduces the training time while guaranteeing a high accuracy.
- We design an intelligent task allocator with the task scheduling and parameter adjustment algorithm, which not only effectively balances the load among different computing nodes but also achieves the accuracy-latency tradeoff.
- We conducted extensive experiments using a real-world prototype and 170-hour surveillance videos. Evaluation results demonstrate that the adaptive cloud-edge SurveilEdge significantly outperforms cloud-only, edge-only, and fixed cloud-edge approaches in terms of query accuracy, bandwidth cost, and query latency.

## II. RELATED WORK

Existing systems on video analytics, such as Chameleon [14], Cherrypick [15], VideoStorm [16] and VideoEdge [21], consider the resource-quality tradeoff and try to find the optimal configuration for delay-sensitive video analytics applications. However, all of them consider general video analytics without concentrating on the query optimizations for surveillance videos. Current video query systems, including Noscope [2], Focus [3], and Blazet [22], conduct specialized optimizations for large-scale video query and improve the query performance significantly using neural networks. However, these works mainly focus on queries of recorded

video datasets rather than real-time queries of video streams as SurveilEdge.

## III. OVERVIEW OF SURVEILEDGE

We first introduce some characteristics observed from real surveillance videos, which are considered in the design of SurveilEdge. Then, we will describe the overall architecture of SurveilEdge.

### A. Spatio-temporal Characteristics of Surveillance Videos

In practice, surveillance cameras that observe the similar sense are likely to produce videos with similar objects. For example, cameras facing a highway and in a building will produce videos of vehicles and persons respectively. In addition, cameras also exhibit periodicity of busy times, which are also different across monitoring senses. These spatio-temporal characteristics are also observed by many works on video analytics [14].

### B. SurveilEdge Overview

We consider a network consisting of cameras, edge devices, and a cloud server, shown in Fig. 2(a). Here, each edge device can serve multiple cameras, communicate with other edge devices, and communicate with the cloud server.

As shown in Fig. 2(b), the workflow of SurveilEdge can be divided into offline and online stages. The offline stage is performed in the Cloud, cameras for similar senses are categorized into different context-specific clusters, each of which produces a context-specific training dataset. At the online stage, when a user inputs a new query command, a CNN with respect to this query will be trained in the cloud, based on the context-specific training dataset established in the offline stage. Therefore, we call this CNN a context and query specific (CQ-Specific) CNN. Here, a CQ-specific CNN is a few-classification CNN which forgoes the full generalization of classifying. However, its model complexity is reduced, and its capability of identifying certain kinds of objects is enhanced. The training process normally takes less than a

minute with a normal Cloud GPU (e.g. NVIDIA Telsa P4). The trained CQ-Specific CNN is then deployed to corresponding edge server. With the CQ-specific CNN at the edge and a highly-accurate CNN(e.g. ResNet-152) in the cloud, each video frame will be processed to produce real-time query responses (normally one to several seconds). SurveilEdge adopts an intelligent scheme for task scheduling and parameter adjustment to balance the system load and the accuracy-latency tradeoffs of queries.

#### IV. SYSTEM DESIGN

This section describe SurveilEdge in detail.

##### A. Camera Clustering and Training Dataset Establishment

Since the query accuracy of specific CNNs highly depends on the training data, an intuitive approach is a specific CNN trained by the images captured by each camera. However, this will cause prohibitively high training cost and latency. Alternatively, it is viable for us to jointly train a specific CNN to serve a cluster of analogous-scene cameras simultaneously. Obviously, the cooperation among analogous-scene cameras also swells the volume of training data for each specific CNN, which can effectively prevent the overfitting caused by small training sets.

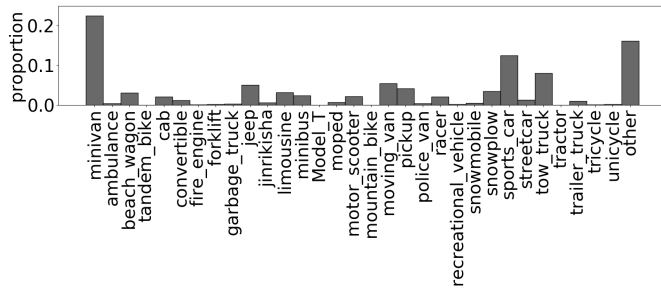


Fig. 3. An example of the profile of a camera (i.e., its proportion vector).

SurveilEdge collects video data at leisure time (without performing query tasks) from each surveillance cameras, where the collected data are processed using highly-accurate CNNs. Particularly, Yolov3 [18] is used to detect common objects in video streams, and ResNet-152 [12] is applied to classify the extracted image of objects and label them, as shown in Fig. 4

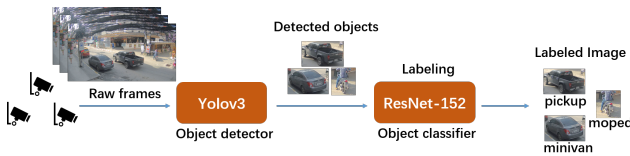


Fig. 4. Illustration of training data labeling.

We use proportion vector to represent the profile of each camera, based on video frames produced by it and uploaded to the Cloud. Each camera profile is computed as the occurrence frequencies of different objects appear in the all video frames captured by this camera. An example of a camera profile is

shown in Fig. 3. Obviously, the camera profile can roughly represent the scene where the camera is deployed. For example, on one hand, if the numbers of cars in two surveillance videos are large, but the proportions of people are very low, then both cameras tend to be near major roads. On the other hand, if there are more people and fewer cars, they tend to be near crowded squares or walking trails.

SurveilEdge computes the profile for every camera, and clusters the cameras (based on their profiles) using the K-Means algorithm [23]. Here, the center of a cluster is also a proportion vector, which are regarded as the profile of this cluster. Cameras within the same cluster are regarded as in the same context, and therefore share the same context-specific training dataset.

##### B. Online Fine-tuning of Query-Specific CNNs

When SurveilEdge receives a new user-defined query command, suitable training data will be selected from the labeled datasets built in the offline stage, using the following method: Firstly, SurveilEdge randomly selects an appropriate number of labeled images of the query objects as the positive training data. Then, the negative training data will be selected from labeled images of non-query objects (i.e., objects do not include the user-defined query commands). For a non-query object, more samples will be selected, if its proportion in the cluster profile is larger. This principle of negative training sample selection will improve the classification accuracy of commonly observed objects.

Next, SurveilEdge fine-tunes a specific CNN, called CQ-specific CNN, based on pre-trained<sup>2</sup> MobileNet [20] and above selected samples. Then, fine-tuning with specific video data enhances learning with a higher starting point while maintaining a smaller learning rate. This allows fast convergence of the loss function to achieve outstanding accuracy on relevant query assignment. For instance, our evaluation shows that it only takes one minute for our fine-tuning scheme to reach more than 92% accuracy with a NVIDIA Tesla P4 GPU. Fig. 5 shows the performances of our specialized training scheme based on the fine-tune technique.

We compared against the method of No Fine-tune (directly using pre-trained weights by ImageNet datasets without fine-tuning), and the method of All Fine-tune (fine-tune for each camera). After the training is accomplished, the weights of specific CNNs are automatically downloaded and deployed on edge devices.

##### C. Moving Object detection and Query Target Recognition

As shown Fig.2 (b), when fine-tuned CQ-CNN achieves enough accuracy, it will be deployed in corresponding edge devices. After then, SurveilEdge will process each video frame to response the user-defined query. Firstly, SurveilEdge determines the presence of moving objects in each frame based

<sup>2</sup>A pre-trained model draws a lot of nutrients from excellent large-scale datasets such as ImageNet and captures universal features like curves and edges.

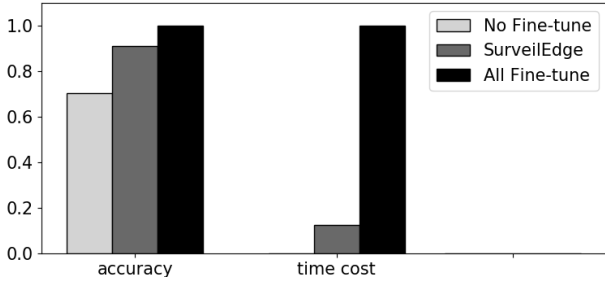


Fig. 5. The performances of different training schemes with a NVIDIA Tesla P4 GPU (already normalized). The accuracy of SurveilEdge almost equals to that of the All Fine-tune but the training time reduces almost 8 $\times$ .

on the frame difference algorithm. The basic idea of the algorithm is as follows: The detector extracts consecutive frames from real-time surveillance video streams with a regular time interval (e.g., one second), and checks the pixel differences between selected frames. If pixels within a certain area change apparently across the frames, it can be considered that a foreground object appears in this area. Detailed operations are as follows.

For a sequence of frames from a video captured by a stationary camera, we extract three consecutive frames  $f_{k-1}(x, y, c)$ ,  $f_k(x, y, c)$ ,  $f_{k+1}(x, y, c)$  to determine the moving objects in frame  $k$ , where  $c$  represents the  $c$ th channel of the image. Then we calculate the per-element absolute differences of successive frames:

$$D_1(x, y, c) = |f_k(x, y, c) - f_{k-1}(x, y, c)| \quad (1)$$

$$D_2(x, y, c) = |f_{k+1}(x, y, c) - f_k(x, y, c)| \quad (2)$$

Next, we calculate the per-element bit-wise logical conjunction:

$$D_a(x, y, c) = D_1(x, y, c) \wedge D_2(x, y, c) \quad (3)$$

Then we convert the color space of the destination image  $D_a(x, y, c)$  into grayscale  $D_g(x, y)$ , and apply a fixed-level threshold to get the binary image  $D_b(x, y)$  for denoising, i.e., filtering out pixels with too small values:

$$D_b(x, y) = \begin{cases} \text{maxval} & \text{if } D_g(x, y) > \text{threshold} \\ 0 & \text{otherwise} \end{cases} \quad (4)$$

where maxval is the maximum value of corresponding image depth, for example 255 for 8-bit grayscale images.

We use some methods of mathematical morphology such as dilation (5) and erosion (6), which have low computation complexity, to remove noises and fill the empty of the target:

$$D_d(x, y) = \max_{x', y' \in \Omega_1} D_b(x + x', y + y') \quad (5)$$

$$D_e(x, y) = \min_{x', y' \in \Omega_2} D_d(x + x', y + y') \quad (6)$$

where  $\Omega_1$  and  $\Omega_2$  represent the neighbourhood of each pixel  $(x, y)$ . Finally, we retrieve object contours from the binary image  $D_e(x, y)$  using the algorithm in [24].

The time interval mentioned above represents the sampling frequency of query, which is denoted by  $s$ . We found that in most scenarios, there is no need to analyze every frame in the video to obtain satisfactory query results. In addition, SurveilEdge discards some detected images with small sizes or imbalances between length and width to avoid wrong detection results caused by disturbance and distinct real movement from noise. Compared with object detection using deep learning algorithms, the frame difference algorithm occupies far less resources and spends much less time with little decay in accuracy.

The detected foreground images and related information including camera ID, capture time, *etc.* are packaged and passed to the task allocator. The allocator performs the task scheduling algorithm and determines the destination of each image among all computing nodes including diverse edge devices and the Cloud. Detailed task scheduling algorithm will be introduced in Subsection IV-D.

Specific CNNs are deployed in edge classifiers and the high-accuracy CNN is deployed in the cloud classifier. When edge classifiers receive an image, they conduct inference and output an identification confidence  $f$  representing the probability that this image is a query object.

- If  $f$  is above the upper threshold  $\alpha$ , this image is confidently considered as a query object.
- If  $f$  is below the bottom threshold  $\beta$ , this image is confidently considered as not a query object.
- If  $f$  is between the bottom threshold  $\beta$  and the upper threshold  $\alpha$ , this image cannot be confidently classified with the CQ-CNN at the edge. In this case, this image will be transmitted to the Cloud and be classified with the highly-accurate CNN (e.g. ResNet-152).

Obviously, the setting of the thresholds has a pronounced influence on the volume of data uploaded to the Cloud, and further affects the computing load of the entire query system. To balance the computing pressure over time, we design a parameter adjustment algorithm to tune the parameter values according to the system load. Detailed parameter adjustment algorithm will be introduced in Subsection IV-E.

#### D. Task Scheduling and Parameter Adjustment

As the spatio-temporal characteristics of surveillance videos we discussed in Subsection III-A, it is reasonable to balance the query load among edge devices with heterogeneous busy time. And due to the periodicity of busy time, the dynamic adjustment of the threshold parameters is beneficial to decide the tradeoff strategy between the latency and the accuracy of queries in different time.

We have  $N$  edge devices, each edge device  $i$  maintains a queue of  $Q_i$  video frames waiting to be classified by itself or be transmitted to another device  $d_i$  for classification. In particular, 0 denotes the Cloud. Let  $t_i$  denotes the inferring time of a detected object (image) for edge device  $i$ <sup>3</sup>.

<sup>3</sup>For simplicity, we ignore transmission time between edge devices. However, it is straightforward to model these latencies in SurveilEdge.

1) *Real-time task scheduling*: For an edge device  $i$ , when an object is detected, the real-time task scheduler will be triggered immediately to determine which device will classify this image with least latency, i.e.

$$d_i = \arg \min_{1 \leq i \leq N} Q_i t_i \quad (7)$$

Each edge device  $i$  maintains a distributed database (SQLite<sup>4</sup> in our implementation) to store parameters including parameters  $\alpha$ ,  $\beta$ , as well as  $t_i$  and  $Q_i$  for all  $i$ . The update of any of these parameters will trigger the immediate update of  $\alpha$ ,  $\beta$ , and  $t_i, \forall i$ .

2) *Real-time updates of  $\alpha$  and  $\beta$* : If the classification latency exceeds the time interval of query, we shrink the interval length of  $[\beta, \alpha]$ . As a result, less images will be uploaded to the Cloud to be classified again. Likewise, if the classification latency does not exceed the time interval of query, the system is capable of reclassifying more images using the highly-accurate CNN on the Cloud to improve the reliability of queries. Therefore, the interval width of  $[\beta, \alpha]$  will be increased, and more images will be transmitted to the Cloud after classification on edges. Meanwhile,  $\alpha$  is limited within the range of  $[0.5, 1]$ , and  $\beta$  is limited within the range of  $[0, 0.5]$ . Specifically,  $\alpha$  is updated as:

$$\alpha_{new} = \max \{ \min \{ \alpha_{old} - \gamma_1 \times (l_d \times t_d - s), 1 \}, 0.5 \} \quad (8)$$

where  $\gamma_1 \in (0, 1)$  is a weighting parameter.  $\beta$  is updated as:

$$\beta_{new} = \gamma_2 \times (1 - \alpha_{new}) \quad (9)$$

where  $\gamma_2$  within  $(0, 1)$  to guarantee that the average of  $\alpha$  and  $\beta$  is lower than 0.5.

It should be more cautious and wary to eliminate an image than regarding this image as a query object. In other words, the recall of query is more important than the precision, since that the query object tends to be sparse in surveillance videos, and missing a query object sometimes can lead to terrible results or even ruin the meaning of query tasks in reality.

3) *Real-time Updates of Estimated Inferring Latency*: To better predict the inferring latencies  $t_i, 1 \leq i \leq N$ , we model the latencies as continuous positive random variables, and apply the skewed distribution, lognormal distribution for the estimation based on recently recorded data. In particular, due to the existence of the minimum latency attributed to the physical limitation, for example the transmission speed limitation determined by the velocity of light, we use the three-parameter lognormal distribution with a support set  $x \in (\gamma, +\infty)$  for some  $\gamma \geq 0$ . The probability density function of the three-parameter lognormal distribution is

$$f(x; \mu, \sigma, \gamma) = \frac{1}{(x - \gamma)\sigma\sqrt{2\pi}} \exp \left\{ -\frac{[\ln(x - \gamma) - \mu]^2}{2\sigma^2} \right\}$$

where  $0 \leq \gamma < x, -\infty < \mu < \infty, \sigma > 0$ , and  $\gamma$  represents the minimum latency in theory. We use  $n$  recently recorded

latency values  $\mathbf{X} = \{x_1, x_2, \dots, x_n\}$  to estimate the parameters of the three-parameter lognormal distribution.

The log-likelihood function is  $\ln L(\mu, \sigma, \gamma | \mathbf{X}) =$

$$-n \ln \sqrt{2\pi} \sigma - \sum_{i=1}^n \ln(x_i - \gamma) - \frac{\sum_{i=1}^n (\ln(x_i - \gamma) - \mu)^2}{2\sigma^2}$$

s. t.  $\min \{x_1, x_2, \dots, x_n\} > \gamma$  (10)

By computing the partial derivatives of the log-likelihood in (10), we can obtain the local maximum likelihood estimating equations:

$$\frac{\partial \ln L}{\partial \mu} = \frac{1}{\sigma^2} \sum_{i=1}^n [\ln(x_i - \gamma) - \mu] = 0 \quad (11)$$

$$\frac{\partial \ln L}{\partial \sigma} = -\frac{n}{\sigma} + \frac{1}{\sigma^3} \sum_{i=1}^n [\ln(x_i - \gamma) - \mu]^2 = 0 \quad (12)$$

$$\frac{\partial \ln L}{\partial \gamma} = \sum_{i=1}^n \frac{1}{x_i - \gamma} + \frac{1}{\sigma^2} \sum_{i=1}^n \frac{\ln(x_i - \gamma) - \mu}{x_i - \gamma} = 0 \quad (13)$$

Then we express the  $\hat{\mu}, \hat{\sigma}^2$  using  $\hat{\gamma}$  by solving (11) (12) (13):

$$\hat{\mu} = \frac{1}{n} \sum_{i=1}^n \ln(x_i - \hat{\gamma}), \quad (14)$$

$$\hat{\sigma}^2 = \frac{1}{n} \sum_{i=1}^n (\ln(x_i - \hat{\gamma}) - \hat{\mu})^2 \quad (15)$$

We replace  $\mu, \sigma$  with estimators (14) (15) in (13) and obtain an equation of  $\gamma$  (16). We solve this equation iteratively and obtain the local maximum likelihood estimator of  $\gamma$ . Naturally, the estimators of  $\mu$  and  $\sigma^2$  can be readily obtained.

$$\left[ \sum_{i=1}^n \frac{1}{x_i - \gamma} \right] \left[ \sum_{i=1}^n \ln(x_i - \gamma) - \sum_{i=1}^n (\ln(x_i - \gamma))^2 + \frac{1}{n} \left( \sum_{i=1}^n \ln(x_i - \gamma) \right)^2 \right] - n \sum_{i=1}^n \frac{\ln(x_i - \gamma)}{x_i - \gamma} = 0 \quad (16)$$

Finally, the expected latency can be regarded as  $E(X) = \hat{\gamma} + \exp\left(\hat{\mu} + \frac{\hat{\sigma}^2}{2}\right)$ . However, using such an approach to estimate the parameters in the three-parameter lognormal distribution, there is a close agreement between  $E(X)$  and  $\bar{x}$ , which sometimes leads to huge swings of latency for outliers. Therefore, in practice, we use the weighted arithmetic mean of  $E(X)$  and  $\text{Median}(X) = \hat{\gamma} + e^{\hat{\mu}}$  to predict the values of latency.

Due to the obvious complexity of the estimation using the three-parameter lognormal distribution, it can only be used to conduct long-periodic latency predictions. Thereby, we design a simple method to decide the value of latency in real time. At first, we initialize the value of latency with an empirical value. Then, we use a self-adaptive weighted mean of the

<sup>4</sup><https://www.sqlite.org/index.html>

historical value  $t_{old}$  and the recently received feedback  $t_{new}$  to dynamically update the value of latency  $t$ :

$$t = \frac{t_{old}^2 + t_{new}^2}{(t_{old} + t_{new})^2} \cdot t_{old} + \frac{2 \cdot t_{old} \cdot t_{new}}{(t_{old} + t_{new})^2} \cdot t_{new} \quad (17)$$

When some extreme values or outliers occur and are returned to the parameter database management system on edge devices, the updating method as (17) can automatically lower the weights of these abnormal values, and thereby reduce their influences on the updated results, which effectively avoids large swings. Obviously, such a prediction method has lower computation complexity than the lognormal method, and can update the latency more frequently. At the same time, the latency estimation method based on the three-parameter lognormal distribution can compensate for the lower reliability of this simple method in longer periods.

## V. EVALUATION

This section present our evaluation of SurveilEdge.

### A. Methodology

**Video Datasets:** We collected real surveillance video streams from YouTube live for the performance evaluation. Specifically, more than 170 hours of video streams from 14 cameras with 1080p resolution and 30 fps frame rate were collected, which covered multiple scenarios such as crossroads, schools and streets. We selected 130 hours of video data for the training of specific CNNs (with Yolov3 for detection and ResNet-152 for classification as stated in III-A). The remaining data were used for evaluation. By applying K-Means clustering on the proportion vectors, the surveillance cameras were divided into two clusters, and two training databases with 140,000 and 75,000 images respectively were determined correspondingly for the training of two specific CNNs.

**Software Tools:** SurveilEdge was implemented in Python on Ubuntu 16.04. Docker containers [25] were adopted for the ease of creation and migration of our distributed system. Opencv [26] and scikit-image [27] were used for image pre-processing and frame difference-based object detection. We used Keras [28] and Tensorflow backend [29] for the implementation of CNN training and inferring, where standard practices (e.g. cross validation and early stopping) were also adopted. For the communication among different nodes, the extremely lightweight publish/subscribe message transport protocol MQTT [30] was adopted. The distributed database management system SQLite was applied on edge devices for database access control. Detailed versions of the adopted tools are listed in Table I.

**Parameter Settings:** We applied MobileNet-v2 as the skeleton of specific CNNs deployed on edge devices, and ResNet-152 as the high-accuracy classifier deployed on the Cloud. Here, the ResNet-152 was treated as the ground-truth CNN for system performance assessment. The query interval was set as 1s for each surveillance video (i.e. sampling once for every 30 frames). We took moped as an instance of query objects for system testing and evaluation. Each edge node was set to

TABLE I  
VERSIONS OF SOFTWARE TOOLS

Software Tools	Versions	Deploy place
Ubuntu	16.04	Edges and Cloud
Docker	18.09.7	Edges and Cloud
Python	3.6.7	Edges and Cloud
OpenCV	4.0.0.25	Edges
Scikit-image	0.14.2	Edges and Cloud
Keras	2.2.4	Edges and Cloud
Tensorflow	1.13.1	Edges and Cloud
Mosquitto	1.6.2	Edges and Cloud
SQLite	3.28.0	Edges

TABLE II  
PERFORMANCES OF 4 QUERY SCHEMES FOR THE SINGLE EDGE AND CLOUD SETTING

	accuracy	average latency	bandwidth cost
<b>SurveilEdge(fixed)</b>	81.56%	2.120s	563.5 MB
<b>SurveilEdge</b>	88.42%	1.018s	1129.5 MB
<b>edge-only</b>	69.03%	2.091s	0 MB
<b>cloud-only</b>	100%	14.823s	3400.3 MB

serve 3-4 surveillance cameras that produce video data and throw them into the query system constantly in real time.

**Comparatives:** For a comprehensive evaluation, we compare the performance of SurveilEdge with that of different solutions.

- **SurveilEdge(fixed):**The cloud-edge system without the task scheduling and parameter adjustment algorithm. For SurveilEdge(fixed), the training scheme and the detection module are the same as SurveilEdge, but all the detected objects are classified by local edge classifiers at first without offloading, and the threshold values remain constant over time, i.e.  $\alpha = 0.8$  and  $\beta = 0.1$ .
- **Edge-only:** All detected object are classified based on CQ-specific CNN without task scheduling.
- **Cloud-only:** All detected object are transmitted to the Cloud and be classified by ResNet-152.

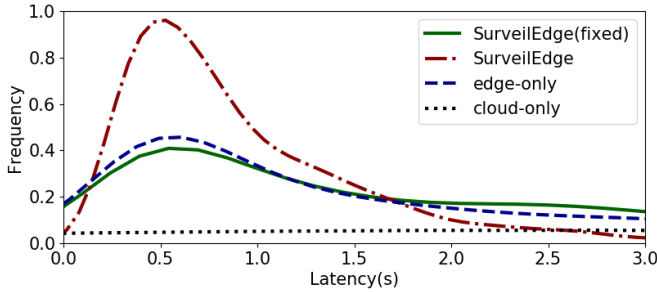
**Performance Metrics:** We use the accuracy, the average latency and the bandwidth cost to evaluate the performance of the aforementioned query schemes including SurveilEdge, SurveilEdge(fixed), the edge-only system and the cloud-only system. Besides these holistic metrics, we also log the query latency of each frame from surveillance video streams to assess the variance of query latency.

We use the F-score to measure the accuracy of queries, which considers both the precision  $p$  and the recall  $r$  of queries. The value of  $F_\lambda$  is calculated as:

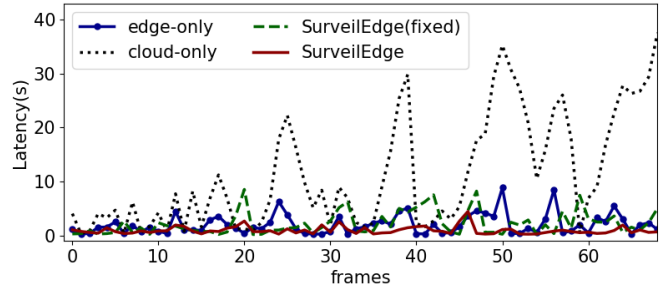
$$F_\lambda = (1 + \lambda^2) \cdot \frac{p \cdot r}{\lambda^2 \cdot p + r}$$

In particular, we set  $\lambda = 2$  and use  $F_2$  measure which emphasizes more on false negatives to assess the accuracy of our prototype, because recall is more crucial than precision for surveillance video query tasks [31].





(a) The PDFs of per frame latency.



(b) The line plots of per frame latency (sampled).

Fig. 6. The performances of four different query schemes for single edge and cloud.

### B. Performance of Single Edge and Cloud

For preliminary tests, we used Docker containers to simulate edge nodes and the Cloud on a server with two Intel Xeon E5-2650v4 CPUs and 512 GB DDR4 RAM. A system with a single edge node and the Cloud was firstly constructed as our primary prototype, where our task scheduling algorithm degraded into the pure cloud-edge scheduling algorithm.

Table. II demonstrates the experimental results under the single edge and cloud setting. As shown in Table. II, compared with the traditional cloud-only query system, SurveilEdge achieved  $3\times$  fewer bandwidth cost,  $14.56\times$  faster query response, and maintained an acceptable query accuracy. Compared with the edge-only query system, SurveilEdge improved the query accuracy by 27.5% and achieved  $2.05\times$  query speedup. The cloud-edge collaborative architecture of SurveilEdge made a good tradeoff between the accuracy and the latency of queries. The classifying and filtering for images on the spot in edge devices reduced the amount of data uploaded to the Cloud and reduced lots of transmission latencies. Meanwhile, the reclassifying mechanism of uploading some images with weak confidences in identification to cloud, compensated the accuracy degradation resulted by classifications using lightweight CNNs in edge devices.

In addition, we recorded the query latency of each frame from surveillance video streams. The Probability Density Functions (PDFs) are shown in Fig. 6 (a), and the line plots are shown in Fig. 6 (b). Obviously, SurveilEdge not only prominently reduced the average latency of the query but more importantly reduced the variance of the query latency. When one computing node was overloaded, the intelligent task allocator would assign next task to the other node with relatively less computing pressure, which avoided the ever-increasing waiting latency. Actually, when the query latency of one frame is too large, the query result of this frame will be out of date and meaningless. And the task allocator enabled more doubtful images to be identified by highly-accurate classifier in cloud during the non-busy time and reduced the uploading volume of data for reclassifying when the whole system was overloaded. The dynamic adjustment of threshold parameters ( $\alpha$  and  $\beta$ ) adaptively balanced the system load and the performance of the query.

TABLE III  
PERFORMANCES OF 4 QUERY SCHEMES FOR THE HOMOGENEOUS EDGES AND CLOUD SETTING

	accuracy	average latency	bandwidth cost
<b>SurveilEdge(fixed)</b>	79.36%	52.295s	574.3 MB
<b>SurveilEdge</b>	90.7%	3.227s	928.9 MB
<b>edge-only</b>	63.55%	51.081s	0 MB
<b>cloud-only</b>	100%	17.698s	3066.9 MB

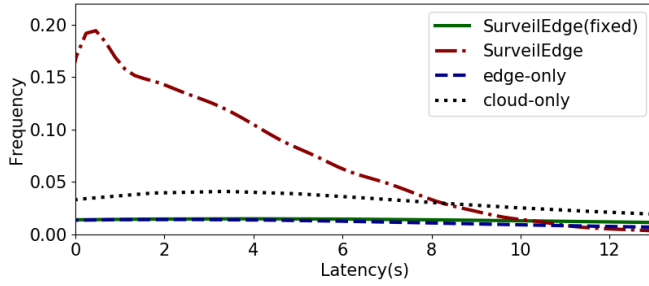
### C. Performance of Homogeneous Edges and Cloud

Considering the satisfactory simulating results under the single edge and cloud setting, we constructed a real-world prototype with three homogeneous edge devices (each with an Intel Core i7-6700 3.4GHz quad core CPU and 16 GB DDR4 RAM) and a public Cloud (with 8 logical cores of Intel Xeon E5-2682v4 CPU, 64 GB DDR4 RAM, and an NVIDIA Tesla P4 GPU) to evaluate the performance of SurveilEdge with the scheduling algorithm integrated.

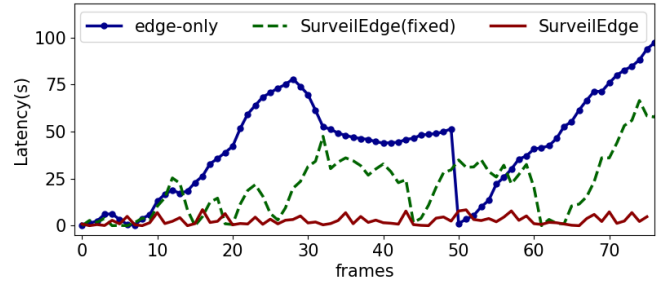
Likewise, the accuracy, the average latency and the bandwidth consumption of different query schemes under the homogeneous edges and cloud setting are shown in Table III. Clearly, compared with the cloud-only query system, SurveilEdge achieved  $3.3\times$  fewer bandwidth cost,  $5.48\times$  faster query response with an acceptable query accuracy, which proved the advantages of cloud-edge collaborative architecture in SurveilEdge again.

Different from the single edge and cloud setting, the resources of edge devices in our prototype under the homogeneous edges and cloud setting were highly fewer than the resources of the Cloud. Correspondingly, we can see that SurveilEdge outperformed the edge-only query system and SurveilEdge(fixed) ( $15.83\times$  and  $16.2\times$  speedup, respectively) more obviously compared with the single edge and cloud setting. The comparison with the SurveilEdge(fixed) also implied the indispensable function of the task allocator in SurveilEdge.

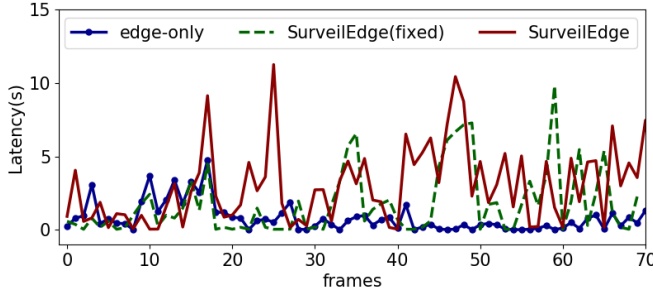
We selected a period of busy time for edge device 1 to further show the effects of the task allocator and drew the line plots of per frame latency on three edge devices in Fig. 7 (b)-(d). We found that the more limited resources of the edge devices made overloading more frequently especially for edge



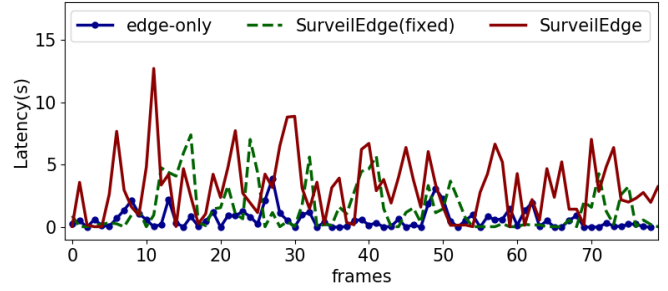
(a) The PDFs of per frame latency.



(b) The line plots of per frame latency on edge device 1 (sampled).



(c) The line plots of per frame latency on edge device 2 (sampled).



(d) The line plots of per frame latency on edge device 3 (sampled).

Fig. 7. The performances of four different query schemes for homogeneous edges and cloud.

device 1 in busy time. The accumulation of query tasks led to ever-increasing queuing time and skyscraping query latency in the edge-only system and SurveilEdge(fixed).

The intelligent task allocator in SurveilEdge offloaded among the edge devices with different busy times and sometimes assigned some tasks to the Cloud when all the edge devices were overloaded. Therefore, by task scheduling, SurveilEdge managed to prevent excessive and anomalous query latency of certain frames, and significantly reduced the average latency of query compared with the edge-only system and SurveilEdge(fixed).

#### D. Performance of Heterogeneous Edges and Cloud

Considering the resource heterogeneity of practical edge devices, we evaluated the performance of SurveilEdge under the heterogeneous edges and cloud setting. With the same system composition as the homogeneous edges and cloud setting, the resource heterogeneity was introduced by respectively limiting the number of logical CPU cores of each edge device, *i.e.* 2, 4 and 8 cores, using the resource virtualization technique of Docker.

According to the detailed results demonstrated in Table IV, it is obvious that SurveilEdge outperformed the cloud-only query system in terms of both the average query latency ( $3.62\times$  speedup) and the bandwidth consumption ( $2.9\times$  fewer). And compared with the edge-only system and SurveilEdge(fixed), SurveilEdge achieved  $10.91\times$ ,  $11.35\times$  speedups of query responses, respectively, and improved the accuracy by 22.4% and 12.3%, respectively.

From the Fig. 8 (b)-(d), we can see that the resource heterogeneity of three edge devices increased the variance of query

TABLE IV  
PERFORMANCES OF 4 QUERY SCHEMES FOR THE HETEROGENEOUS EDGES AND CLOUD SETTING

	accuracy	average latency	bandwidth cost
<b>SurveilEdge(fixed)</b>	75.3%	117.23s	609.2 MB
<b>SurveilEdge</b>	86.9%	10.33s	1100.5 MB
<b>edge-only</b>	67.5%	112.79s	0 MB
<b>cloud-only</b>	100%	37.42s	3197.7 MB

latency, larger than that under the homogeneous edges and cloud setting, in the edge-only system and SurveilEdge(fixed). Edge device 2 and 3 had relatively more resources and fewer burdens of the query tasks, which resulted in less query latency. However, the lack of computing power on edge device 1 made the accumulation of the tasks worse and brought larger waiting latency.

By the observation of Fig. 8 (b)-(d), we find that in SurveilEdge, the edge device 2 and 3 shared the query tasks on the edge device 1 under the control of the task allocator. The cooperation among the edge devices with different busy times improved the resource utilization of the whole query system and avoided excessive queuing time. Therefore, both the mean value and variance of query latency were reduced prominently in SurveilEdge.

## VI. CONCLUSION AND FUTURE WORKS

In this paper, we present a cloud-edge collaborative and real-time query system, SurveilEdge, for large-scale surveillance video streams, which significantly reduces the query latency and the bandwidth cost while guaranteeing an acceptable accuracy. Moreover, the intelligent task allocator with the



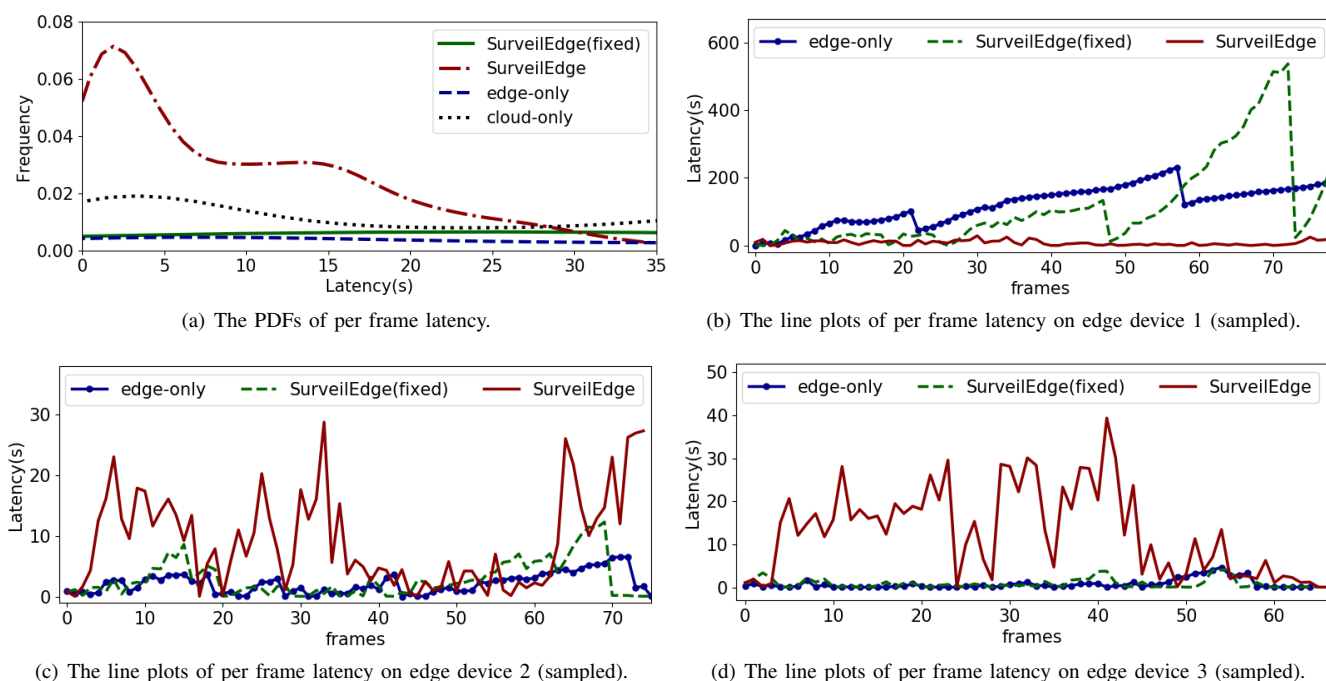


Fig. 8. The performances of four different query schemes for heterogeneous edges and cloud.

task scheduling and parameter adjustment algorithm manages to balance the system load and reduce the variance of per frame query latency. We implement SurveilEdge on the real-world prototype with a public Cloud and multiple homogeneous/heterogeneous edge devices for the performance evaluation based on real surveillance videos. Experimental results demonstrate the effectiveness and advantages of our approach. In fact, our schemes and system architecture are not limited to the particular use case in this paper, and they can be beneficial to most latency-sensitive applications based on deep learning. We will be pursuing a better tradeoff among latency, bandwidth cost and accuracy for broadened latency-sensitive applications in future.

## REFERENCES

- [1] IHS Markit, "Security technologies top trends for 2019," <https://cdn.ihs.com/www/pdf/1218/IHSMarkit-Security-Technologies-Trends-2019.pdf>.
- [2] D. Kang, J. Emmons, F. Abuzaid, P. Bailis, and M. Zaharia, "Noscope: optimizing neural network queries over video at scale," *PVLDB*, vol. 10, no. 11, pp. 1586–1597, 2017.
- [3] K. Hsieh, G. Ananthanarayanan, P. Bodik, S. Venkataraman, P. Bahl, M. Philipose, P. B. Gibbons, and O. Mutlu, "Focus: Querying large video datasets with low latency and low cost," in *Proc. USENIX OSDI*, 2018, pp. 269–286.
- [4] G. Ananthanarayanan, P. Bahl, P. Bodik, K. Chintalapudi, M. Philipose, L. Ravindranath, and S. Sinha, "Real-time video analytics: The killer app for edge computing," *Computer*, vol. 50, no. 10, pp. 58–67, 2017.
- [5] K. Su, J. Li, and H. Fu, "Smart city and the applications," in *ICECC*. IEEE, 2011, pp. 1028–1031.
- [6] L. Wang and D. Sng, "Deep learning algorithms with applications to video analytics for A smart city: A survey," *CoRR*, vol. abs/1512.03131, 2015. [Online]. Available: <http://arxiv.org/abs/1512.03131>
- [7] P. Kumar, S. Ranganath, H. Weimin, and K. Sengupta, "Framework for real-time behavior interpretation from traffic video," *IEEE T INTELL TRANSP*, vol. 6, no. 1, pp. 43–53, 2005.
- [8] Y. Tang, C. Zhang, R. Gu, P. Li, and B. Yang, "Vehicle detection and recognition for intelligent traffic surveillance system," *MULTIMED TOOLS APPL*, vol. 76, no. 4, pp. 5817–5832, 2017.
- [9] Y. LeCun, Y. Bengio, and G. Hinton, "Deep learning," *nature*, vol. 521, no. 7553, p. 436, 2015.
- [10] A. Krizhevsky, I. Sutskever, and G. E. Hinton, "Imagenet classification with deep convolutional neural networks," in *NIPS*, 2012, pp. 1097–1105.
- [11] S. Ren, K. He, R. Girshick, and J. Sun, "Faster r-cnn: Towards real-time object detection with region proposal networks," in *NIPS*, 2015, pp. 91–99.
- [12] K. He, X. Zhang, S. Ren, and J. Sun, "Deep residual learning for image recognition," in *Proc. IEEE CVPR*, 2016, pp. 770–778.
- [13] K. He, G. Gkioxari, P. Dollár, and R. Girshick, "Mask r-cnn," in *Proc. IEEE ICCV*, 2017, pp. 2961–2969.
- [14] J. Jiang, G. Ananthanarayanan, P. Bodik, S. Sen, and I. Stoica, "Chameleon: scalable adaptation of video analytics," in *Proc. ACM Sigcomm*. ACM, 2018, pp. 253–266.
- [15] O. Alipourfard, H. H. Liu, J. Chen, S. Venkataraman, M. Yu, and M. Zhang, "Cherry-pick: Adaptively unearthing the best cloud configurations for big data analytics," in *Proc. USENIX NSDI*, 2017, pp. 469–482.
- [16] H. Zhang, G. Ananthanarayanan, P. Bodik, M. Philipose, P. Bahl, and M. J. Freedman, "Live video analytics at scale with approximation and delay-tolerance," in *Proc. USENIX NSDI*, 2017, pp. 377–392.
- [17] S. Venkataraman, Z. Yang, M. Franklin, B. Recht, and I. Stoica, "Ernest: efficient performance prediction for large-scale advanced analytics," in *Proc. USENIX NSDI*, 2016, pp. 363–378.
- [18] J. Redmon and A. Farhadi, "Yolov3: An incremental improvement," *arXiv*, 2018.
- [19] M. Satyanarayanan, "The emergence of edge computing," *Computer*, vol. 50, no. 1, pp. 30–39, 2017.
- [20] A. G. Howard, M. Zhu, B. Chen, D. Kalenichenko, W. Wang, T. Weyand, M. Andreetto, and H. Adam, "Mobilenets: Efficient convolutional neural networks for mobile vision applications," *CoRR*, vol. abs/1704.04861, 2017. [Online]. Available: <http://arxiv.org/abs/1704.04861>
- [21] C.-C. Hung, G. Ananthanarayanan, P. Bodik, L. Golubchik, M. Yu, P. Bahl, and M. Philipose, "Videoeage: Processing camera streams using hierarchical clusters," in *Proc. IEEE/ACM SEC*. IEEE, 2018, pp. 115–131.

- [22] D. Kang, P. Bailis, and M. Zaharia, "Blazeit: Fast exploratory video queries using neural networks," *arXiv preprint arXiv:1805.01046*, 2018.
- [23] J. A. Hartigan and M. A. Wong, "Algorithm as 136: A k-means clustering algorithm," *Journal of the Royal Statistical Society. Series C (Applied Statistics)*, vol. 28, no. 1, pp. 100–108, 1979.
- [24] S. Suzuki *et al.*, "Topological structural analysis of digitized binary images by border following," *Computer vision, graphics, and image processing*, vol. 30, no. 1, pp. 32–46, 1985.
- [25] D. Merkel, "Docker: lightweight linux containers for consistent development and deployment," *Linux Journal*, vol. 2014, no. 239, p. 2, 2014.
- [26] G. Bradski, "The OpenCV Library," *Dr. Dobb's Journal of Software Tools*, 2000.
- [27] S. van der Walt, J. L. Schönberger, J. Nunez-Iglesias, F. Boulogne, J. D. Warner, N. Yager, E. Gouillart, T. Yu, and the scikit-image contributors, "scikit-image: image processing in Python," *PeerJ*, vol. 2, p. e453, 6 2014. [Online]. Available: <https://doi.org/10.7717/peerj.453>
- [28] F. Chollet *et al.*, "Keras," <https://keras.io>, 2015.
- [29] M. Abadi, P. Barham, J. Chen, Z. Chen, A. Davis, J. Dean, M. Devin, S. Ghemawat, G. Irving, M. Isard *et al.*, "Tensorflow: A system for large-scale machine learning," in *Proc. USENIX OSDI*, 2016, pp. 265–283.
- [30] R. A. Light *et al.*, "Mosquito: server and client implementation of the mqtt protocol." *J. Open Source Software*, vol. 2, no. 13, p. 265, 2017.
- [31] C. J. V. Rijsbergen, *Information Retrieval*, 2nd ed. Newton, MA, USA: Butterworth-Heinemann, 1979.